Desalination and Water Treatment
www.deswater.com

doi: 10.5004/dwt.2019.23439

140 (2019) 290–301
February

Pb(II) removal from wastewater by modified activated carbon in batch and fixed-bed column studies: synthetic and real wastewater application

Aloysius Akaangee Pam[a,b,*], Abdul Halim Abdullah[a], Yen Ping Tan[a], Zulkarnain Zainal[b]

[a]*Chemistry Department, Faculty of Science, Universiti Putra Malaysia, 43400 UPM Serdang, Selangor Darul Ehsan, Malaysia, emails: aloysius.pam@fulokoja.edu.ng (A.A. Pam), halim@upm.edu.my (A.H. Abdullah), typ@upm.edu.my (Y.P. Tan)*
[b]*Chemistry Department, Faculty of Science, Federal University Lokoja, P.M.B. 1154, Lokoja, Nigeria, email: zulkar@upm.edu.my (Z. Zainal)*
[c]*Material Synthesis and Characterization Laboratory, Institute of Advanced Technology, Universiti Putra Malaysia, 43400 UPM Serdang, Selangor Darul Ehsan, Malaysia*

Received 19 January 2018; Accepted 6 November 2018

ABSTRACT

Activated carbon (AC) prepared from palm kernel was modified by citric acid (CA) to enhance its ability for Pb(II) removal from aqueous solutions. The product obtained was characterized using energy dispersive X-ray spectroscopy, Brunauer-Emmett-Teller method, Fourier transform infrared, spectroscopy, and field emission scanning electron microscope (FESEM). The adsorption of Pb(II) ions onto CA modified activated carbon (AC-CA), was studied in both batch and column mode operations. In the batch studies, a wide range of operating parameters, such as adsorbent dose (0.1–0.95 g), initial metal ion concentration (50–150 mg/L), contact time (15–150 min), and pH (1–5), were investigated. Equilibrium data were fitted using Langmuir, Freundlich, first and second order kinetic models. The experimental data were best characterized by pseudo-second order kinetic model and Langmuir isotherm models; indicative of chemisorption and monolayer adsorption, respectively. ACs and AC-CA were mainly microporous with pores in the range of 1.2–1.76 nm. Although the surface area of AC-600 (1,559.9 m^2/g) was much higher than that of AC-CA (1,267.1 m^2/g), the Pb(II) sorption capacity of AC-CA was larger than that of AC-600. The AC and AC-CA, both showed high Q_{max} of 81.0 and 103.1 mg/g, the high adsorption capacity of the adsorbents is promising in the development of low cost and novel adsorbent. It is concluded that Pb(II) ions removal using palm kernel shells based adsorbent modified with citric acid would be an efficient technique for economic treatment of wastewater.

Keywords: Activated carbon; Activation; Palm kernel shell; Characterization; Lead; Breakthrough time

1. Introduction

Pollution of water bodies by heavy metals has negative consequences on both the environment and human health. Among the different metals, lead is the most important toxic heavy element in the environment [1] released into the natural waters from different manufacturing activities. Its use is associated with more than 900 industries, including mining, smelting, refining, battery manufacturing, and so on [2]. Lead is a greatly poisonous metal that can do great harm to almost every organ in the body [1]. Of all the organs, the nervous system is the frequently affected target in lead toxicity, both in children and adults [1]. Therefore, it is imperative to reduce the level of Pb(II) ions in wastewater. Various removal methods have been proposed for treatment of Pb contaminated water (e.g., precipitation, adsorption, membrane separation, and ion exchange). Among these different methods, adsorption is one of the methods predominately applied for the removal of metal ions in wastewater due to its economic and efficient nature. Adsorption methods offer the advantages of

---

[*] Corresponding author.

simple operation, low cost, and low secondary environmental pollution and can be applied to remove heavy metals at less than 100 mg/L when other methods cannot work effectively [3]. The application of activated carbon for environmental protection has gained remarkable interest in recent times due to the distinctive properties, such as well-developed pore structure and high surface area [4]. Palm kernel shell, one of the most abundant agro-industrial by-products, has demonstrated good sorption capabilities for different adsorbates. For example, palm kernel shells (PKS) based activated carbon (AC) was synthesized and used in the removal of Pb(II) [5–7], methane [8], fluoride [9], Cd(II), and Zn(II). Activated carbon also requires complexing agents to improve its removal performance for inorganic matters [10]. Because citric acid was an effective chelating agent, it was used in this work for the modification of the AC. Although a number of studies have examined the application of PKS adsorbent in the treatment of Pb(II) in solution, adsorption of Pb(II) onto PKS-derived AC involving competitive and reusability studies, application in real wastewater and in continuous column in addition to modification with citric acid has not been sufficiently reported yet.

In view of the aforementioned, the aim of this study was to investigate the feasibility of using citric acid functionalized PKS-activated carbon (AC-CA) as adsorbent for Pb(II) removal from wastewater. The objective of this study is to examine the effect of citric acid on physicochemical properties of AC, and evaluate the potential use of AC-CA in the removal of Pb(II) in both batch and fixed bed adsorption.

2. Experimental setup

2.1. Preparation of activated carbon

Activated carbon was prepared from palm kernel shell by chemical method using concentrated orthophosphoric acid (H_3PO_4, 85%; Merck, Darmstadt, Germany). PKS residues, obtained from the Malaysian Palm Oil Board, were used after crushing, washing with distilled water and drying under the sun. The PKS powder and H_3PO_4 in a ratio 2:1 g/g (acid to PKS), were mixed and manually stirred intermittently for about 30 min and dried in an oven at 110°C for 24 h. The samples were carbonized at 500°C and 600°C at a heating rate of 10°C/min for 1 h in a vertical tubular furnace under nitrogen flow of 20 mL/min. The resulting activated carbons (AC-500 and AC-600) were washed thoroughly with warm deionized water until the pH of the wash water was constant, filtered and dried in the oven at 110°C for 24 h. The ACs were passed through 200 – mesh sieve before used for characterization and applications in adsorption tests of Pb(II).

2.2. Characterization of adsorbents

The specific surface area and porosity data of the treated PKS were determined from nitrogen adsorption desorption isotherm using surface analyzer (Autosorb-1, Quantachrome, Boynton Beach, FL, USA) using the Brunauer-Emmett-Teller (BET) equation and Barrett–Joyner–Halenda (BJH) method, respectively. The elemental composition was investigated using energy dispersive X-ray spectroscopy (EDS) integrated with high-resolution FEI Nova 230 field emission scanning electron microscope (FESEM). The samples were then placed onto aluminum stubs by means of carbon tape placed on the stub. The samples were gold coated to prevent charging. The samples were then transferred into the vacuum chamber and observed at magnifications in the ranges of 1,500× to 10,000×.

The point of zero charge (pHpzc) of the ACs was assessed using the pH drift method [11].

2.3. Adsorbent screening experiment

The screening experiments were accomplished using the batch method. This was achieved by introducing 0.1 g of each of the adsorbents into 250 mL (50 mg/L) of Pb and agitating for 120 min at room temperature to reach equilibrium. The mixture was filtered using 0.45 μm microporous membrane. The concentration of the Pb(II) in the filtrate was analyzed using Atomic absorption spectroscopy (AAS). Experiments were performed in triplicates and results analyzed at aggregate level.

2.4. Preparation of citric acid-modified activated carbon

Modification of the optimum adsorbent (AC-600) was performed using citric acid. This was achieved by introducing 5 g each of AC-600 into different concentrations of citric acid (0.1–0.3 M, 100 mL solution); the resulted mixture was refluxed at 60°C for 2 h. Thereafter, the modified activated carbon, AC-CA, was filtered and under sonication, washed with warm distilled water for 10 min to eliminate any excess citric acid salt, and finally, dried at 100°C for 24 h.

2.5. Batch adsorption studies

The desired working concentrations were obtained by diluting the stock solution of Pb(II) (1,000 mg/L) that was obtained by dissolving the required amount of lead nitrate (Fisher scientific) into 1,000 mL ultrapure water.

Sorption experiment was performed by the batch method to assess both the rate and equilibrium data. To investigate the effect of sorbent dose on the equilibrium uptake of Pb(II), adsorbent masses of 0.1–0.95 g was used. The effect of pH was studied by adjusting the pH of the Pb(II) solution to the desired values at the range of 1–5 using 0.1 M NaOH and 0.1 M HCl and measured by a pH meter (Sartorius PB-10). Isotherms studies were investigated by varying the initial Pb(II) solution concentration from 50 to 150 mg/L. For the kinetic study, 250 mL of 120 mg/L of Pb(II) solutions was added to known amount of adsorbent and agitated for 20 min. The effect of temperature was also studied in a range of 25°C–60°C in a temperature-controlled water bath (Memmert, Germany), under optimal conditions. To investigate the competitive effect, mixtures of Pb(II), Cu(II) and Zn(II) ions and 0.25 g of AC-CA was introduced to a solution (250 mL) containing the same concentration of individual metal ion (50 mg/L), having different combinations of Pb(II)–Cu(II), Pb(II)–Zn(II), and Pb(II)–Cu(II)–Zn(II), respectively. To examine the reusability, the Pb-loaded AC-CA was regenerated in 1.0 M HCl and HNO_3 solution. The regenerated AC-CA recyclability test was assessed by dispersing it in fresh 250 mL of the Pb(II) solution and agitating at rate of 160 rpm for 250 min. At any given time intervals, an aliquot of the mixture was withdrawn and the concentration of the metal ions was measured using atomic adsorption spectrophotometer (Thermo Scientific-S series). Percentage removal (%) and metal ions adsorbed per unit mass of AC-CA (q_t) were computed as follows:

$$q_e = (C_o - C_e)V/m \tag{1}$$

$$\text{Efficiency (\%)} = (C_o - C_e)/C_o \times 100 \tag{2}$$

where C_o and C_e are the initial and equilibrium concentrations (mg/L), V is the volume of solution used, and m is the mass of adsorbent (g).

2.6. Column study

Fixed bed experiments were conducted using a glass column of 2 cm internal diameter. The column was packed with 3.5 and 7.0 g of AC-CA to give bed heights of 2.5 and 4.3 cm, respectively, with a layer of glass wool and acid wash sand positioned at the bottom. 150 mg/L of Pb(II) solution was pumped through the packed column with the aid of a peristaltic pump to maintain constant flow rates of 10 and 15 mL/min in a down-flow mode at room temperature. At predetermined intervals, the effluent samples were taken and evaluated. The column experiments were brought to a halt when the column attained exhaustion.

2.7. Real sample analysis

Adsorptions studies using real samples solutions obtained from Sungai Balok River, Pahang, and from an electroplating plant in Selangor, both in Malaysia, were conducted by batch experiments. The water samples were filtered to eliminate suspended particles and stored in plastic bottles for further experiments. AAS was used to analyze the initial metal ion concentration in the water samples. Owing to the relative low concentration of the metal ions in the river water, the sample was spiked with 50 mg/L of Pb(II) in 250 mL solution. For the electroplating wastewater, it was used without spiking. The wastewater was treated under optimum conditions obtained based on the preliminary experiments, on that basis; 0.25 g of the AC-CA was dispersed in 250 ml of effluent solution at 50°C and pH 4 for 150 min. The solution was filtered at the end of the experiment and the remaining concentration of Pb(II) was determined.

3. Results and discussion

3.1. Screening and modification results

Fig. 1(a) shows the screening experiment results of the activated carbons. The synthesized ACs demonstrated excellent adsorption behaviour towards Pb(II). The adsorption capacity obtained from the adsorbents was 43.6 mg/g (AC-500) and 58.9 mg/g (AC-600) for 50 mg/L of Pb. Hence, the AC-500 was not considered for further Pb(II) adsorption experiments, instead, emphases was placed on A-600 as the main adsorbent in all adsorption experiments.

Experiments were carried out to determine the optimum conditions for chemical modification of AC-600. It can be seen that the 0.20 M is the most appropriate modification concentration for the citric acid used (Fig. 1(b)). The adsorption efficiency of modified activated carbon was influenced by the concentration of citric acid in the sequence of 0.2 M > 0.1 M > activated carbon (AC-600) > 0.30 M. The corresponding adsorption capacities were 121.6, 108.0, 100.5, and 82.5 mg/g, respectively. Further increase in the citric acid loading on AC-600 up to 0.3 M, reduced the performance. This is because excess amount of citric molecules escaped from the adsorbent into the solution, forming CA–Pb(II) complexes which were difficult to be sorbed by the AC due to higher molecular weight. Zou et al. [12] reported similar trend for the removal of Cu(II) onto EDTA functionalized $CoFe_2O_4$ with similar claims for decrease in Cu(II) adsorption after a certain EDTA concentration was attained. Based on these results, AC-CA 0.2 was selected for further experiments involving batch and column studies.

3.2. Physicochemical characterization of AC-PKS and AC-CA

Table 1 shows the BET surface area and pore size distributions of AC-500, AC-600 and the modified AC-CA computed using the BJH method. The average pore size distributions showed that the adsorbents are microporous in nature with average micropore size in the range of 1.53 to 1.92 nm. The higher amount of nitrogen adsorbed at low relative pressure revealed the presence of predominant micropores in

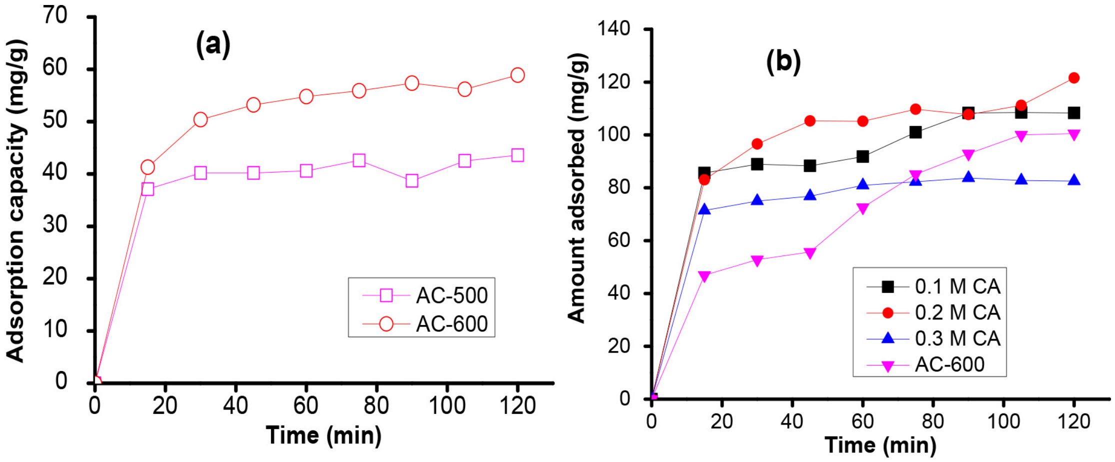

Fig. 1. Screening experiments of (a) AC-500 and AC–600, (b) modified AC-600 (100 mg/L of Pb, adsorbent dosage = 0.1 g).

Table 1
Surface area and porosity of activated carbon

Sample	S_{BET}(m^2/g)	Micropore volume (V_{mic}, cm^3/g)	Microspore size (nm)	Microspore surface area ($S_{mic,}$$m^2$/g)
AC-500	1,267.1	0.264	1.53	169.26
AC-600	1,559.9	0.303	1.71	139.74
AC-CA 0.1	1,155.7	0.60	1.71	193.7
AC-CA 0.2	860.407	0.233	1.70	142.42
AC-CA 0.3	749.164	0.377	1.92	265.26

the adsorbent structure (Fig. S1). From the results presented in Table 1 for the BET surface area and pore structure for AC-500, AC-600, and AC-CA, it is clearly seen that the BET surface areas of AC-CAs were slightly lower than that of AC-600. This could be due to the blockage of internal porosity occasioned by the formation of new functional groups at the mouth of the pores upon modification with citric acid. The FESEM images clearly revealed that the surface texture of the ACs under study has no marked differences in their morphologies before and after the modification process (Fig. S2).

The different elemental constituents of the ACs as recorded from the energy dispersive X-ray spectroscopy analysis showed that the carbon surface consists mainly of elemental phosphorus (11.1%), oxygen (13.9%), and carbon (75.0%). The point of zero charge of the activated carbons, which was estimated to be 3.5–4.0 (figure not presented in the paper), shows that the adsorbents have acidic surfaces and the introduction of citric acid does not significantly change the surface properties of AC-600. It is, therefore, anticipated that the adsorbents surface would be positively charged at pH below 3.9 and negatively charged at pH 4.0 and above.

3.3. Effect of adsorption parameters on Pb(II) removal

3.3.1. Effect of adsorbent dosage

Figs. 2(a) and (b) show the effect of AC-600 and AC-CA dosage on the removal of Pb(II). There was a greater removal efficiency of Pb(II) by AC-600 and AC-CA for dosage in the range of 0.1–0.35, however, only slight increases in the range 0.36–0.95. Bearing in mind, the adsorption efficiency and economy, 0.35 g of AC-600 and 0.25 g AC-CA was selected as the optimum adsorbent dosage in subsequent batch experiments.

3.3.2. Effect of contact time

The effect of contact time represents the optimum time for the complete removal of Pb(II) [13] onto AC-600 and (b) AC-CA adsorbents as presented Fig. 3. It was observed that the adsorption efficiency of Pb(II) removal increased rapidly with contact time at the initial stage for the first 60 min in both adsorbents. The fast adsorption at the initial stage of the adsorption process was due to the large amount of the sorption sites which provide the driving force for faster transfer of the Pb(II) onto the absorbents surfaces, but then gradually decreased as the surface sites became saturated and equilibrium was obtained. From the results, the equilibrium time was fixed at about 120 min for AC-600 and 140 min for AC-CA for the Pb concentration used.

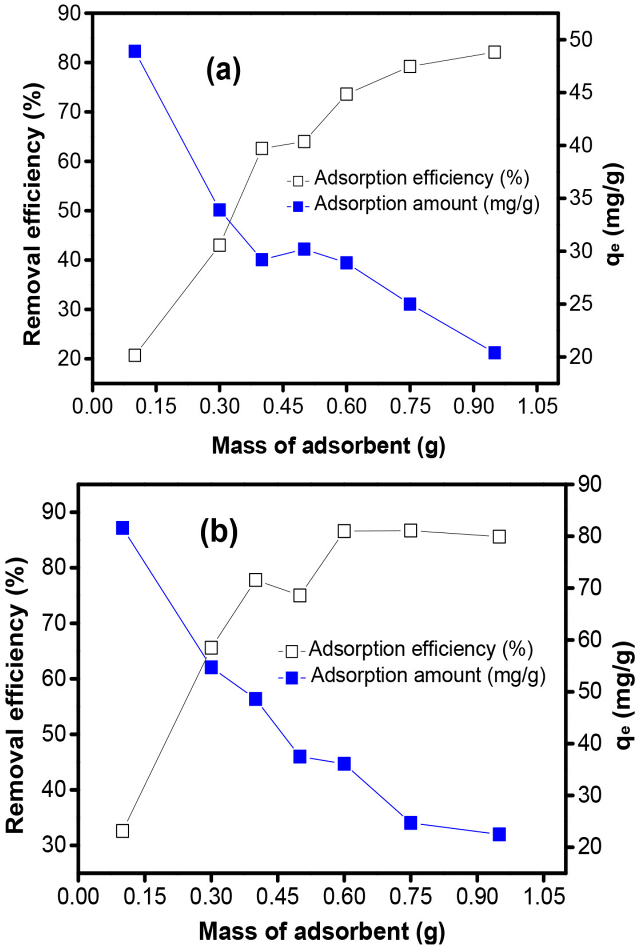

Fig. 2. Effect of AC-600 and AC-CA dose on the sorption removal efficiency of Pb(II) from solution (Pb(II) concentration = 100 mg/L; volume = 250 mL; adsorption time = 120 min; adsorbent dosage = 0.1–0.95 g).

3.3.3. Effect of pH

The dependence of metal adsorption on pH is directly related to both the ionization state of the functional groups and metal chemistry in the solution, which affects the accessibility of binding sites [14]. Fig. 4 reveals the effect of pH on adsorption of Pb(II) from aqueous solution onto the adsorbents. The results showed that the removal efficiency of the Pb(II) ions increased remarkably with the increasing pH value up to 4, but did not change significantly when increased to pH 5 for AC-600, however, showed a drastic decrease for AC-CA. The results can be explained based on the surface

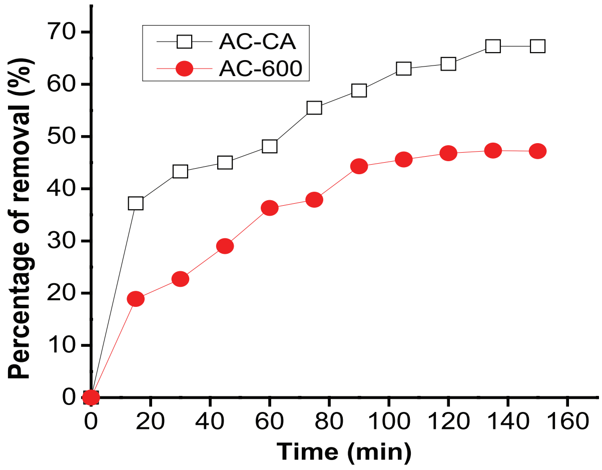

Fig. 3. Effect of contact time on Pb(II) adsorption by AC-600 and AC-CA (final equilibrium pH = 3.37; Pb(II) = 100 mg/L; adsorbent dosage = 0.35 g; temperature =25°C ± 1°C, and contact time = 160 min).

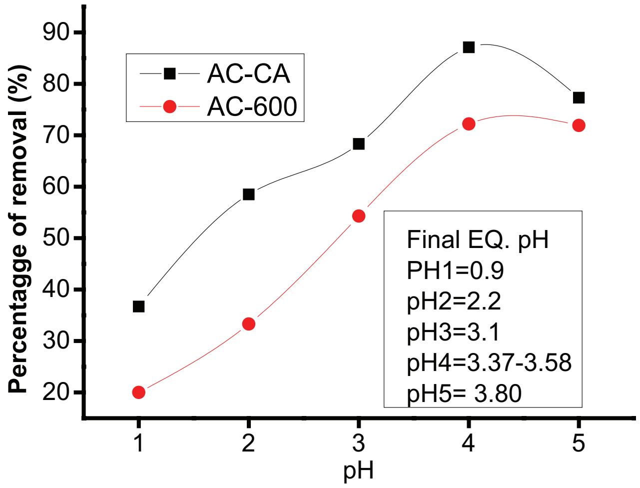

Fig. 4. Effects of pH on the adsorption of Pb(II) onto AC-600 and AC-CA (adsorbent dosage = 0.35 g/250 mL, AC-600 and 0.25 g/250 mL, AC-CA; Pb(II) = 150 mg/L).

charge and competition between Pb(II) and H_3O^+. Within the range of 4–5, the Pb(II) ions were effectively removed and this correlated with the surface charge of the ACs. The pHpzc is established around 3.9 for both AC-600 and AC-CA; the adsorbent surfaces are bound to be positively charged at pH < 4 and negatively charged at pH > 4. Adsorption efficiency was found to be low at pH < 4.0 because of the abundant H_3O^+ or H^+ ions that competed with Pb(II) ions for available binding sites. At pH 4, maximum amount of Pb(II) uptake recorded was 72.2% and 87.1% (AC-600 and AC-CA), respectively, which can be attributed to the electrostatic attraction between the negatively charged surface of the adsorbents and Pb(II) ions.

3.3.4. Adsorption isotherm, kinetics and thermodynamics

Langmuir and Freundlich isotherm models were employed to explain the interaction between the equilibrium concentration of Pb(II) in solution and its uptake on AC-600 and AC-CA when both the phases are in equilibrium. The Langmuir and Freundlich isotherm models can be represented as Eqs. (3) and (4) [15] as follows:

$$\frac{C_e}{q_o} = \frac{1}{q_m b} + \frac{C_e}{q_m} \tag{3}$$

$$\text{In}q_e = \text{In}K_F + \frac{1}{n}\text{In}C_e \tag{4}$$

A plot of C_e/q_e vs C_e gives a straight line with slope of $1/q_m$ and intercept $1/q_m b$. C_e and q_e represent concentration (mg/L) and the amount (mg/g) of metal adsorbed at equilibrium, respectively, q_m (mg/g) and b (L/mg) are constants relating to maximum adsorption capacity and adsorption energy, respectively.

Langmuir isotherm plot was also expressed in relation to separation factor (R_L), which is defined by the following relationship:

$$R_L = 1/1 + bC_0 \tag{5}$$

The equilibrium adsorption capacity of the AC-600 and AC-CA towards Pb(II) were evaluated using the adsorption isotherms with different initial Pb(II) concentrations varying from 50 to 150 mg/L at 25°C under pH conditions (pH 5.0). The relationship of Pb(II) uptake (q_e) with Pb(II) equilibrium concentration (C_e) (Fig. 5(a)) inferred that the sorption of Pb(II) by AC-600 and AC-CA, increased with increase of Pb(II) equilibrium concentrations. The reason is that higher initial concentration provides the necessary driving force to overcome the resistance of Pb(II) ions between the aqueous and solid phase [16]. It could be observed from Fig. 5(a) and Table 2 that more Pb(II) was sorbed on AC-CA than that of AC-600. This is due to the relatively higher density of binding sites on the AC-CA caused largely to the effect of CA introduced.

The various parameters obtained for the fitness of Freundlich and Langmuir equilibrium models are presented in Table 2. Based on the correlation coefficient (R^2), the adsorption isotherm data could be better explained by Langmuir isotherm equation than by Freundlich isotherm equation. The maximum amount of Pb adsorbed ($q_{\max}$) was 81 mg/g of AC-600 and 103 mg/g of AC-CA. The separation factor was less than 1 in all cases, indicating favourable adsorption of Pb(II) onto AC-600 and AC-CA.

The comparison of maximum Pb(II) adsorption capacity on AC-600 and AC-CA with some activated carbon-based adsorbents previously reported in literature is given in Table 3. The results revealed that AC-600 and AC-CA showed an enhanced adsorption capacity than other activated carbon from agriculture wastes.

To identify the mechanism governing the overall sorption rate of Pb(II), the experimental data was applied to different kinetic models, including the pseudo-first order, pseudo-second order and intraparticle diffusion. Eqs. (6) and (7) give the linearized form of the pseudo-first order and pseudo-second order kinetic models [18] as follows:

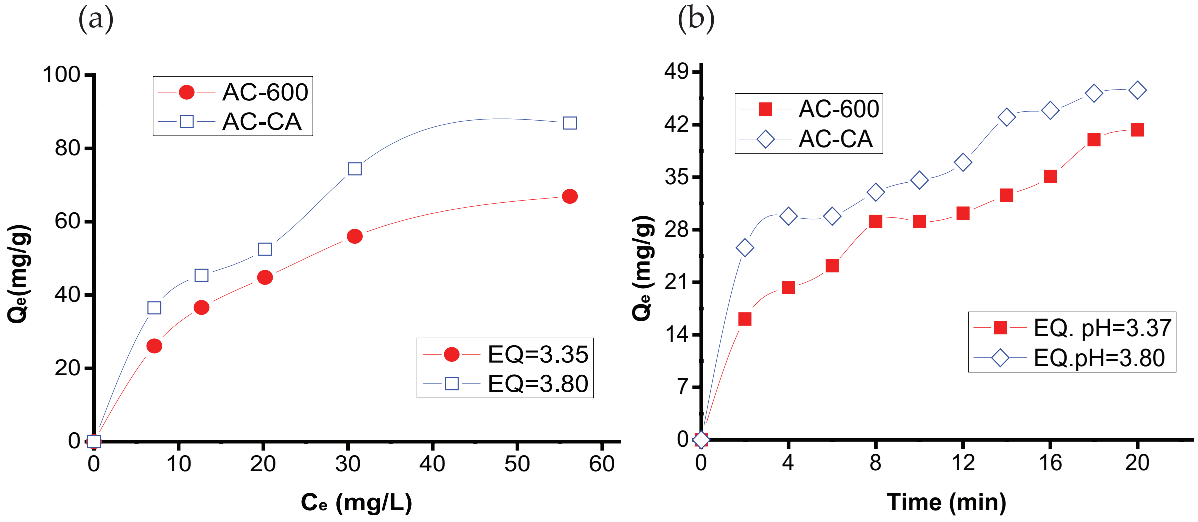

Fig. 5. (a) Adsorption isotherms of Pb(II) onto AC-600 and AC-CA (temperature = 25°C ± 1°C). (b) Sorption kinetics of Pb(II) by AC-600 and AC-CA (Pb(II) = 120 mg/L; temperature = 25°C ± 1°C).

Table 2
Langmuir and Freundlich isotherm constants and coefficients of determination for Pb(II) adsorption onto AC-600 and AC-CA

Adsorbents	Langmuir isotherm				Freundlich isotherm		
	Q_{max} (mg/g)	b	R_L	R^2	K_F	n	R^2
AC-600	81.0±0.45	1.209	0.0054	0.9805	1.256± 0.45	2.271	0.9559
AC-CA	103±0.34	0.0002	0.9649	0.9660	1.237±0.41	1.77	0.8586

Table 3
Comparison of maximum adsorption capacities (Q_m) of Pb(II) ions by different adsorbents

Adsorbent	Experimental conditions			(mg/g)	Reference
	pH	Dosage (g)	Concentration (mg/L)		
PKS activated carbon (AC)	4.0	0.35	50–150	81.0	This study
PKS AC modified with AC-CA	4.0	0.25	50–150	103.1	This study
Coconut shell AC	4.5	0.05	50	26.50	[17]
Polygonum orientale Linn AC	5.0	0.6	50–75	50–75	
Apricot stone AC	6	1.0		21.38	[18]
Raffia palm fruit epicarp AC	6	0.5	100–700	28.0–66.37	[19]
Coconut shell AC	5.5	1.0	5–50	26.14–49.92	[20]
Palm shell	4.5	0.005	25–400	419.9	[7]
Corncob	–	–	–	298.5	[21]

$$\ln(q_e - q_t) = \ln q_e - k_1 t \tag{6}$$

$$\frac{t}{q_t} = \frac{1}{K_2 q_e^2} + \frac{1}{q_e} t \tag{7}$$

where k_1 (min^{-1}), k_2 (g mg^{-1} min^{-1}), q_e (mg/g), and q_t (mg/g) are the first-order rate constant, pseudo-second order rate constants, the amounts of metal ions adsorbed at equilibrium at any given time, respectively.

Fig. 5(b) shows the adsorption kinetics of Pb(II) by AC-600 and AC-CA as a function of time. The sorption process was rapid during the initial 19 min, and adsorption equilibrium was attained approximately 20 min. It follows from Table 4 that the kinetic data best fitted to the pseudo-second order kinetic equation. The values of the correlation coefficient (R^2) are higher than those obtained with the pseudo-first order equation and the calculated q_e values are also in good agreement with experimental values, thus suggesting that the adsorption process is governed by chemisorption rather than involvement of mass transfer in the bulk solution [13,22].

The intraparticle diffusion model for the sorption of Pb(II) onto AC-600 and AC-CA is represented in Eq. (8) as follows:

$$Q_t = K_d t^{1/2} + C \tag{8}$$

where K_d is the intraparticle diffusion rate constant (mg/g min$^{1/2}$) and C is the intercept. The plots for Pb(II) adsorption onto AC-600 and AC-CA as presented in Figs. 6(a) and (b), respectively, exhibited multi-linearity with three different stages. The first stage is attributed to faster Pb(II) migration from the bulk solution to external surface of the adsorbents, termed external diffusion [21,24]. The second stage relates to the gradual adsorption stage, corresponding to Pb(II) diffusion inside the pores of the adsorbent, where intraparticle diffusion is rate-controlled, while the third section is attributed to the final equilibrium stage [23].

As presented in Fig. 6, none of the straight lines passed through the origin of the plot. This indicates that the film diffusion as well as intraparticle diffusion occurred simultaneously during the Pb(II) sorption on AC-600 and AC-CA. Thus, the adsorption of Pb(II) ions onto AC-600 and AC-CA surface is complex, comprising more than one mechanism [20].

Figs. 7(a) and (b) show the extent of Pb(II) adsorption onto AC-600 and AC-CA with increase of temperature. It was found that the amount adsorbed increased with temperature, indicating the adsorption process was endothermic in nature. However, the sorption capacity slightly decreased over 50°C. It is possible that the temperature was sufficient to cause higher rate of desorption than that of adsorption. To that effect, the determination of thermodynamic parameters was restricted to solution temperature of 25°C–50°C.

The change in free energy ($\Delta G°$), enthalpy $\Delta H°$, and entropy $\Delta S°$ associated with the adsorption process was calculated by using the following equations:

$$\Delta G^\circ = -RT\,\mathrm{In}K_C \tag{9}$$

$\Delta H°$ and $\Delta S°$ were calculated from Van't Hoff's equation shown below:

$$\mathrm{In}K_C = \left(\frac{\Delta S^\circ}{R}\right) - \left(\frac{\Delta H^\circ}{R}\right)\frac{1}{T} \tag{10}$$

where K_C is the equilibrium constant, and R is the universal gas constant (8.314J/mol K). $\Delta H°$ and $\Delta S°$ were determined from the slope and intercept of linear plot of InK_C and $1/T$, respectively (Fig. 7(b)). The calculated $\Delta G°$ values are as presented in Table 5. The negative values of $\Delta G°$ is an indication of the spontaneous nature of the adsorption process [24]. The positive values of $\Delta H°$ (AC-CA = 20.1, AC-600 = 33.9) kJ/mol and $\Delta S°$ (AC-CA = 64.0, AC-600 = 121.9) J/mol. K confirmed the endothermic nature of adsorption process and could suggest an increase in degree of freedom at the solid/liquid interface during the adsorption process, respectively.

3.3.5. Real water sample

The adsorbent performance in real wastewater was investigated using water samples taken from river water (Sungai Balok river, Pahang) and effluent from an electroplating industry located in Selangor, Malaysia. Table 6 shows the concentrations of Pb, Zn, Cu, and Ni that was present in the river water and electroplating effluent. The maximum WHO

Table 4
Pseudo-first order and pseudo-second order constants and coefficients of determination for Pb(II) adsorption onto AC-600 and AC-CA

Adsorbent	Pseudo-first order				Pseudo-second order		
	q_e exp (mg/g)	q_e calc (mg/g)	k_1 (min^{-1})	R^2	Q_e calc (mg/g)	k_2 (g/mg min)	R^2
AC-600	39.4±0.50	1.05	0.1795	0.7263	48.1±0.41	0.037	0.9634
AC-CA	46.6±0.02	1.23	0.2063	0.7789	53.7±0.01	0.0049	0.9703

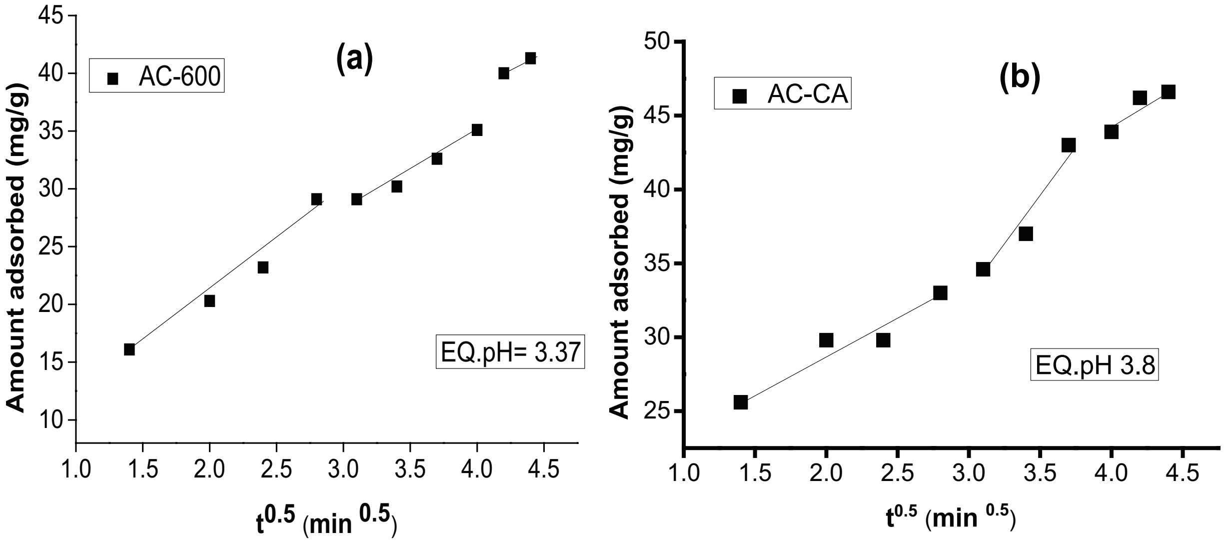

Fig. 6. Intraparticle kinetic modelling for Pb adsorption onto (a) AC-600 and (b) AC-CA for different initial concentrations of Pb (Pb(II) C_o = 120 mg/L; temperature = 25°C ±1°C).

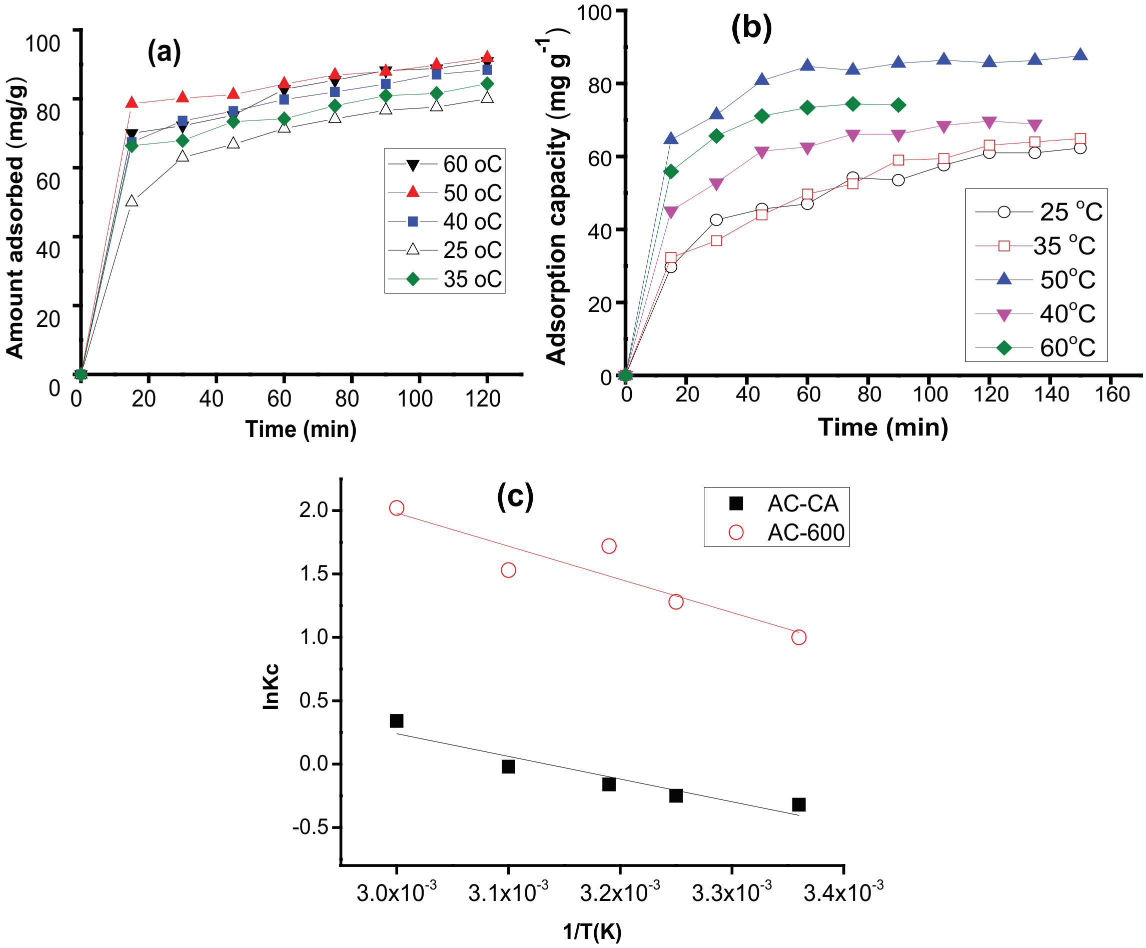

Fig. 7. Effect of temperature on Pb(II) adsorption on (a) AC-CA and (b) AC-600. (c) Thermodynamic plot of Pb(II) adsorption onto AC-600 and AC-CA (adsorbent dosage = 0.35 g/250 mL, AC-600 equilibrium pH = 3.5, and 0.25 g/250 mL, AC-CA; equilibrium pH = 3.85).

Table 5
Thermodynamic parameters for the adsorption of Pb(II) onto AC-600 and AC-CA at various temperatures

Temperature (K)	AC-600			AC-CA		
	Q (mg/g)	ln*K*	Δ*G*° (kJ/mol)	*Q* (mg/g)	ln*K*	Δ*G*° (kJ/mol)
298	80.0±0.23	1.00	–2.478	62.3±0.28	–0.32	0.793
308	84.4±0.44	1.28	–3.278	64.9±0.06	–0.25	0.640
313	88.4±0.14	1.75	–4.55	67.2±0.99	–0.16	0.416
323	91.5±0.86	2.02	–4.307	87.6±0.19	0.34	–0.913
333	90.9±0.36	1.85	–5.010	72.6±0.31	–0.02	0.055

permissible limit for Pb, Zn, and Cu is 0.05, 5.0, and 1.0 mg/L, respectively [25]. The result showed that Pb was slightly above the maximum WHO allowable limits of 0.05 mg/L in river water but was relatively high in electroplating wastewater. As shown in Table 6, the AC-CA effectively removed the Pb(II) and Zn(II) ions from the water samples. It should be noted that the adsorption capacity of AC-CA in removing 50 mg/L synthetic Pb(II) solution was 45.4 mg/g (91.4%). The decrease in sorption capacity in the river samples (spiked samples) compared with those present in deionized water could be attributed to the presence of heavy metals such as Pb(II), Zn(II), Cu(II), and Ni(II) (Table 6) in river samples, which as a result could impede the effective removal of Pb(II).

The adsorption capacity electroplating wastewater was 78.5 mg/g for Pb (91.7%), 2.44 mg/g for Cu (35.7%), and 6.2 mg/g for Zn (95.6%). The adsorbents showed effective removal of Pb(II) in electroplating samples despite the relatively high level of Pb(II) in it compared with the river water. This could be due to more metals ions (Cu, Zn, and Ni) present in the river water compared with electroplating wastewater (Cu and Zn).

Table 6
Results of spiked water samples and electroplating effluent

Metal ions	River water				Electroplating effluent		
	Pb(II)	Zn(II)	Cu(II)	Ni(II)	Pb(II)	Zn(II)	Cu(II)
Concentration (mg/L)	0.06	0.05	0.03	0.04	81.9	6.2	6.8
% Removal	70.2[a]	nd	nd	nd	91.7	95.6	35.7
Adsorption capacity (mg/g)	35.1[a]	nd	nd	nd	78.5	6.2	2.44

[a]Results for spiked water sample
nd, not tested.

3.3.6. Competitive adsorption

The competitive effect of Pb, Cu, and Zn on the adsorption process on AC-CA is illustrated in Fig. 8. In the single-solute adsorption, the order of the adsorbent affinity towards the metals was Pb(II) > Cu(II) > Zn(II). In multiple solute mixture, the selective coefficient Q/Q was used to account for the effect of multiple metal adsorption [26], where Q and Q represent adsorption amount in single and multimetal mixture, respectively. Since Q/Q ratio was <1, the coexistence of Pb(II), Cu(II), and Zn(II) in both binary and ternary showed strong antagonism thereby reducing the adsorption capacity of the individual metal ions, indicating that there is competitive sorption between the heavy metals in the mixture as their removal was affected by the presence of the other metals. Sdiri et al. [27] also reported similar phenomenon.

3.3.7. Reusability properties of AC-CA

The regeneration of the biosorbent is an important key factor in examining the potential of the biosorbent for commercial application [28]. The decrease in uptake capabilities of AC-CA Pb(II) after three successful cycles was 2.2%, 30.1%, and 35.2% (HCl), and 2.2%, 32.1%, and 36.8% (HNO_3) (Fig. S3). This decrease in removal efficiency of Pb(II) could be due to deformation of the pore structure or some of the trapped Pb(II) molecules in the pore after desorption with the acids. Since the AC-CA is predominantly microporous; in the dimension range 1.71–1.92 nm, there is high tendency for such pore to be easily obstructed. Therefore, the reusability potential of the AC-CA may not be practicable beyond the third cycle.

3.3.8. Analysis of breakthrough experimental data

The performance of a packed bed for adsorption of Pb(II) was described through breakthrough curve in order to assess the practical utility of the AC-CA, for continuous treatment of the Pb(II) – laden effluents on an industrial scale operation, and to estimate the binding capacity of the adsorbent. The total quantity of Pb(II) adsorbed in the column (Q_{total}) for a given feed concentration (C_o) and flow rate (F) can be computed from the following equation:

$$q_e(\text{mg}) = \frac{F}{1000}\int_{t=0}^{t=t_b}(C_o - C_e)\,\text{d}t \qquad (11)$$

where (C_o – C_t) is the amount of adsorbed Pb(II) ion and F the flow rate (mL/min).

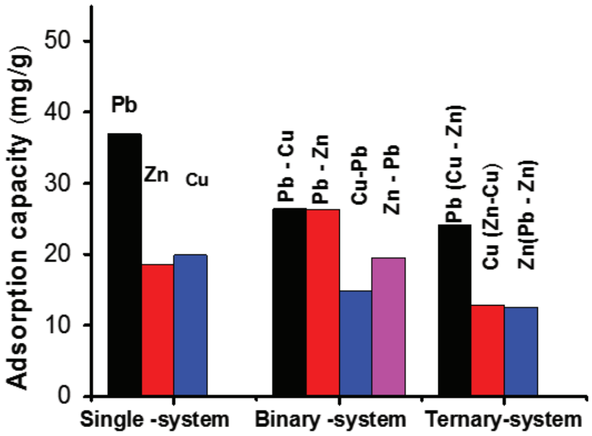

Fig. 8. Effect of coexisting cationic ions on the Pb(II) ions adsorption onto AC-CA (t = 2 h 30 min; AC-CA dose, 0.25 g/250 mL; C_o = 50 mg/L; temperature = 25°C ± 1°C; shaken speed = 160 rpm).

The approach by Shukor et al. [29] was adopted for computing the column capacity for the adsorption of Pb(II). Breakthrough capacity $q_{e\,10\%}$ (C_e/C_i = 0.1) stated in mg of Pb(II) adsorbed per gram of AC-CA was determined using Eq. (12):

$$q_{e\,10\%} = Q_{\text{total}}/M \qquad (12)$$

Fig. 9(a) shows the effect of the feed flow rate on the adsorption of Pb onto AC-CA. The breakthrough curves for the fast flow rate showed relatively early t_b (the time required to attach the breakthrough point, in min) and t_e (the time required for completion, in min) of the adsorption, consequently, resulting in less adsorption capacity. This may be due to the inadequate residence time for the Pb(II) ions within the bed and the partial diffusivity of the solute into the adsorptive sites or pores of the AC-CA [30]. Lower flow rates offered longer residence time with high adsorption capacity. Similar observations were made in literature [31,32].

Fig. 9(b) represents the bed height effects on the adsorption performance of AC-CA. The s-shape and the gradient of plotted breakthrough curves for the two heights differ slightly, with both t_b and t_e values increasing as the bed depth increased, which led to higher adsorption capacity of Pb(II) onto AC-CA (Table 7). This was ascribed to longer mass transfer zone [33] and availability of more adsorption sites. The result is similar to previous fixed-bed column studies, which reported increase in adsorption of Pb(II) with increase

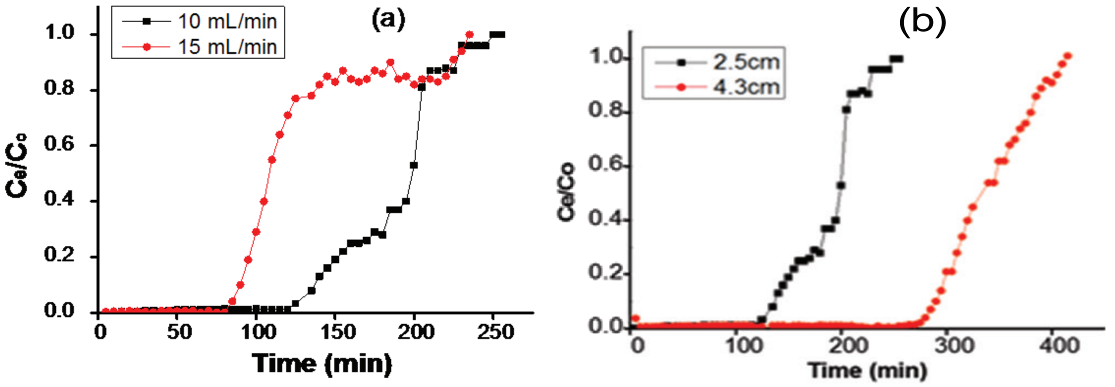

Fig. 9. Breakthrough curves for adsorption by Pb(II) onto AC-CA at (a) different flow rates (Pb(II) = 150 mg/L; bed height = 2.5 cm) and (b) bed height (flow rate = 10 mL/min).

Table 7
Breakthrough parameters for Pb(II) adsorption onto AC-CA

Column condition			Breakthrough analysis	
C_o (mg/L)	Bed height (cm)	Flow rate (mL/min)	t_b (min)	Uptake Q(mg/g)
150	4.3	10	320	68.6±0.43
150	2.5	10	190	58.1±0.02
150	2.5	15	85	54.6±0.03

in heights [34,35]. Table 7 presents the column adsorption capacity for Pb(II) onto the AC-CA at different operating parameters, including bed height, flow rate, and feed concentration.

Adsorption capacity of AC-CA in column was less than that in the batch method. This difference could be credited to the duration of batch processes and solid/solution ratio selection [36,37]. Goel et al. [38] obtained similar results for removal of Hg(II) from water by coconut shell activated carbon, and attributed it to potential irreversibility of the sorption process and the various approaches to adsorption equilibrium in the two systems. Nevertheless, the column adsorption capacity was higher than 22–54 mg reported for concentration of 500–1,000 mg/L of Pb [34].

4. Conclusion

Based on the analysis conducted on the AC-600 and AC-CA, Pb(II) could be successfully treated from wastewater using these absorbents. The BET results have shown a decrease in microspore volume and change in textural properties after surface modification of AC-600. The modified sample showed enhanced adsorption capacity than the AC-600. Adsorption of Pb(II) onto AC-600 and AC-CA both followed Langmuir adsorption isotherm models while kinetic data fitted best on pseudo-second order model. Moreover, the intraparticle diffusion of Pb(II) ions into the micropores was governed by more than one mechanism. Adsorption capacity for 150 mg/l inlet concentration of Pb(II) at the column operational rate of 10 L/min and bed height of 4.3 cm was found to be 68.6 mg/g. The results of Q_{max} computed in this work were at par or showed comparably higher value with published literature. In addition, the synthesized adsorbents demonstrated good regeneration capacity in three successful adsorption/desorption tests. Therefore, AC-600 and AC-CA adsorbents are promising adsorbents for Pb(II) treatment in contaminated wastewater in both batch and continuous systems.

References

[1] A.L. Wani, A. Ara, J.A. Usmani, Lead toxicity: a review, Interdiscip. Toxicol., 8 (2015) 55–64.
[2] A.T. Jan, M. Azam, K. Siddiqui, A. Ali, I. Choi, Q.M.R. Haq, Heavy metals and human health: mechanistic insight into toxicity and counter defense system of antioxidants, Int. J. Mol. Sci., 16 (2015) 29592–29630.
[3] C. Tang, Y. Shu, R. Zhang, X. Li, J. Song, B. Li, et al., Comparison of the removal and adsorption mechanisms of cadmium and lead from aqueous solution by activated carbons prepared from *Typha angustifolia* and *Salix matsudana*, RSC Adv., 7 (2017) 16092–16103.
[4] S. Shi, X. Zhou, W. Chen, M. Chen, T. Nguyen, X. Wang, W. Zhang, Improvement of structure and electrical conductivity of activated carbon by catalytic graphitization using N_2 plasma pretreatment and iron(iii) loading, RSC Adv., 7 (2017) 44632–44638.
[5] Z. Yi, J. Yao, H. Chen, F. Wang, X. Liu, J. Xu, Equilibrium and kinetic studies on adsorption of Pb(II) by activated palm kernel husk carbon, Desal. Wat. Treat., 57 (2016) 7245–7253.
[6] F.T. Ademiluyi, E.O. David-West, Effect of chemical activation on the adsorption of heavy metals using activated carbons from waste materials, ISRN Chem. Eng., 2012 (2012) 1–5.
[7] C.E. Choong, S. Ibrahim, Y. Yoon, M. Jang,.Removal of lead and bisphenol A using magnesium silicate impregnated palm-shell waste powdered activated carbon: comparative studies on single and binary pollutant adsorption, Ecotoxicol. Environ. Saf., 148 (2018) 142–145.
[8] S.S.A. Syed-Hassan, M.S. Zaini, Optimization of the preparation of activated carbon from palm kernel shell for methane adsorption using Taguchi orthogonal array design, Korean J. Chem. Eng., 32 (2016) 1–11.
[9] A.H.B.A. Bakar, Y.S. Koay, Y.C. Ching, L.C. Abdullah, T.S.Y. Choong, M. Alkhatib, et al., Removal of fluoride using quaternized palm kernel shell as adsorbents: equilibrium isotherms and kinetics studies, BioResources, 11 (2016) 4485–4511.
[10] S. Babel, Low-cost adsorbents for heavy metals uptake from contaminated water: a review, J. Hazard. Mater., 97 (2003) 219–243.

[11] L. Wang, J. Li, Removal of methylene blue from aqueous solution by adsorption onto crofton weed stalk, BioResources, 8 (2013) 2521–2536.

[12] Z. Zou, Z. Shi, L. Deng, Highly efficient removal of Cu(II) from aqueous solution using a novel magnetic EDTA functionalized $CoFe_2O_4$, RSC Adv., 7 (2017) 5195–5205.

[13] M. Arshadi, M.J. Amiri, S. Mousavi, Kinetic, equilibrium and thermodynamic investigations of Ni(II), Cd(II), Cu(II) and Co(II) adsorption on barley straw ash, Water Resour. Ind., 6 (2014) 1–17.

[14] A.A. Farghali, M. Bahgat, A.A. Enaiet, M.H. Khedr, Adsorption of Pb(II) ions from aqueous solutions using copper oxide nanostructures, Beni-Suef Univ. J. Basic Appl. Sci., 2 (2013) 61–71.

[15] M. Rafatullah, O. Sulaiman, R. Hashim, A. Ahmad, Removal of cadmium(II) from aqueous solutions by adsorption using meranti wood, Wood Sci. Technol., 46 (2012) 221–224.

[16] V. Patrulea, A. Negrulescu, M. Mincea, L. Pitulice, O. Spiridon, V. Ostafe, Optimization of the removal of copper (II) ions from aqueous solution on chitosan and cross-linked chitosan beads, BioResources, 8 (2013) 1147–1165.

[17] M. Sekar, V. Sakthi, S. Rengaraj, Kinetics and equilibrium adsorption study of lead(II) onto activated carbon prepared from coconut shell, J. Colloid Interface Sci., 279 (2004) 307–313.

[18] L. Mouni, D. Merabet, A. Bouzaza, L. Belkhiri, Adsorption of Pb(II) from aqueous solutions using activated carbon developed from apricot stone, Desalination, 276 (2011) 148–153.

[19] J.N. Ghogomu, S.N. Muluh, D.L. Ajifack, A.A.B. Alongamo, D.T. Noufame, Adsorption of lead (II) from aqueous solution using activated carbon prepared from Raffia palm (*Raphia Hookeri*) fruit epicarp, IOSR J. Applied Chem., 9 (2016) 74–85.

[20] G.E. Sharaf El-Deen, S.E.A. Sharaf El-Deen, Kinetic and isotherm studies for adsorption of Pb(II) from aqueous solution onto coconut shell activated carbon, Desal. Wat. Treat., 57 (2016) 28910–28931.

[21] Q. Liu, Properties of chemically prepared corncob-based activated carbons and their adsorption characteristics for aqueous lead and phenol, Desal. Wat. Treat., 72 (2017) 197–206.

[22] W. Rudzinski, W. Plazinski, On the applicability of the pseudo-second order equation to represent the kinetics of adsorption at solid/solution interfaces: a theoretical analysis based on the statistical rate theory, Adsorption, 15 (2009) 181–192.

[23] C. Song, S. Wu, M. Cheng, P. Tao, M. Shao, G. Gao, Adsorption studies of coconut shell carbons prepared by KOH activation for removal of lead(II) from aqueous solutions, Sustainability, 6 (2014) 86–98.

[24] Z.Y. Yao, J.H. Qi, L.H. Wang, Equilibrium, kinetic and thermodynamic studies on the biosorption of Cu(II) onto chestnut shell, J. Hazard. Mater., 174 (2010) 137–143.

[25] K.G. Akpomie, F.A. Dawodu, Treatment of an automobile effluent from heavy metals contamination by an eco-friendly montmorillonite, J. Adv. Res., 6 (2015) 1003–1013.

[26] F. Bouhamed, Z. Elouear, J. Bouzid, B. Ouddane, Multi-component adsorption of copper, nickel and zinc from aqueous solutions onto activated carbon prepared from date stones, Environ. Sci. Pollut. Res., 23 (2016) 15801–15806.

[27] A. Sdiri, T. Higashi, R. Chaabouni, F. Jamoussi, Competitive removal of heavy metals from aqueous solutions by montmorillonitic and calcareous clays, Water Air Soil Pollut., 223 (2012) 1191–1204.

[28] A. Pandey, D. Bera, A. Shukla, L. Ray, Studies on Cr(VI), Pb(II) and Cu(II) adsorption-desorption using calcium alginate as biopolymer, Chem. Speciat. Bioavailab., 19 (2007) 17–24.

[29] A. Shukor, A. Aziz, L. Abd, H.C. Man, Column dynamic studies and breakthrough curve analysis for Cd(II) and Cu(II) ions adsorption onto palm oil boiler mill fly ash (POFA), Environ. Sci. Pollut. Res., 1 (2014) 1–12.

[30] S. Muthusamy, S. Venkatachalam, Competitive biosorption of Cr(VI) and Zn(II) ions in single- and binary-metal systems onto a biodiesel waste residue using batch and fixed-bed column studies, RSC Adv., 5 (2015) 45817–45826.

[31] V.C. Taty-Costodes, H. Fauduet, C. Porte, Y.S. Ho, Removal of lead (II) ions from synthetic and real effluents using immobilized *Pinus sylvestris* sawdust: adsorption on a fixed-bed column, J. Hazard. Mater., 123 (2005) 135–144.

[32] M.K. Mondal, Removal of Pb(II) ions from aqueous solution using activated tea waste: adsorption on a fixed-bed column, J. Environ. Manage., 90 (2009) 3266–3271.

[33] Z.Z. Chowdhury, S.B.A. Hamid, R. Das, M.R. Hasan, S.M. Zain, K. Khalid, et al., Preparation of carbonaceous adsorbents from lignocellulosic biomass and their use in removal of contaminants from aqueous solution, BioResources, 8 (2013) 6523–6555.

[34] R. Lakshmipathy, N.C. Sarada, A fixed bed column study for the removal of Pb(II) ions by watermelon rind, Environ. Sci. Water Res. Technol., 1 (2015) 244–250.

[35] J.L. Gong, Y.L. Zhang, Y. Jiang, G.M. Zeng, Z.H. Cui, K. Liu, et al., Continuous adsorption of Pb(II) and methylene blue by engineered graphite oxide coated sand in fixed-bed column, Appl. Surf. Sci., 330 (2015) 148–157.

[36] S. Treumann, S. Torkzaban, S.A. Bradford, R.M. Visalakshan, D. Page, An explanation for differences in the process of colloid adsorption in batch and column studies, J. Contam. Hydrol., 164 (2014) 219–229.

[37] G. Sadeghi, J.F. Schijven, T. Behrends, S.M. Hassanizadeh, M.T. Van Genuchten, Bacteriophage PRD1 batch experiments to study attachment, detachment and inactivation processes, J. Contam. Hydrol., 152 (2013) 12–17.

[38] J. Goel, K. Kadirvelu, C. Rajagopal, Mercury (II) removal from water by coconut shell based activated carbon: batch and column studies, Environ. Technol., 25 (2004) 141–153.

Supplemental material

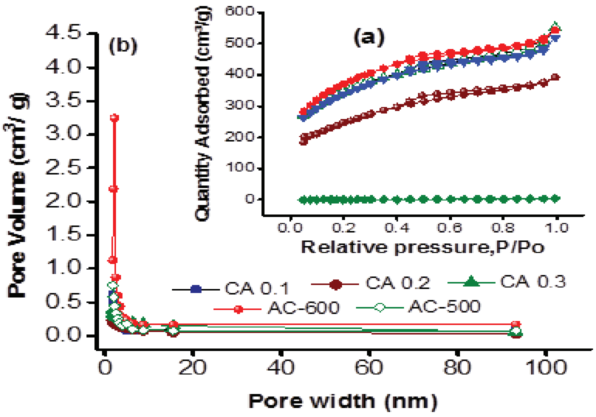

Fig. S1. (a) N_2 adsorption isotherm and (b) pore size distribution for AC-PKS and AC-CA.

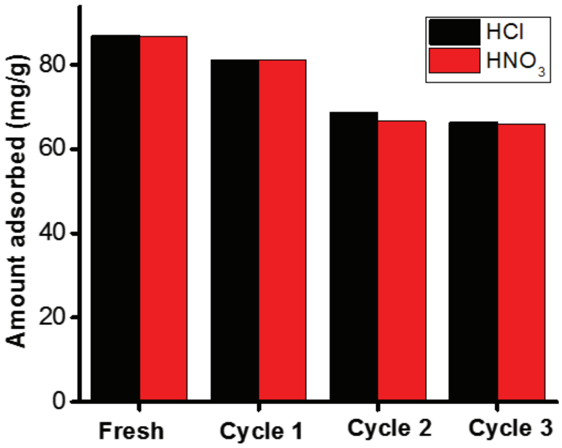

Fig. S3. Adsorption capacity Pb(II) uptake and recovery in successive cycles using 1M HCl and HNO_3 (t = 2h.30min; Pb(II) C_0 = 150 mg/L; ads. dosage = 0.25 g /250 mL, and temp. = 25 1°C)

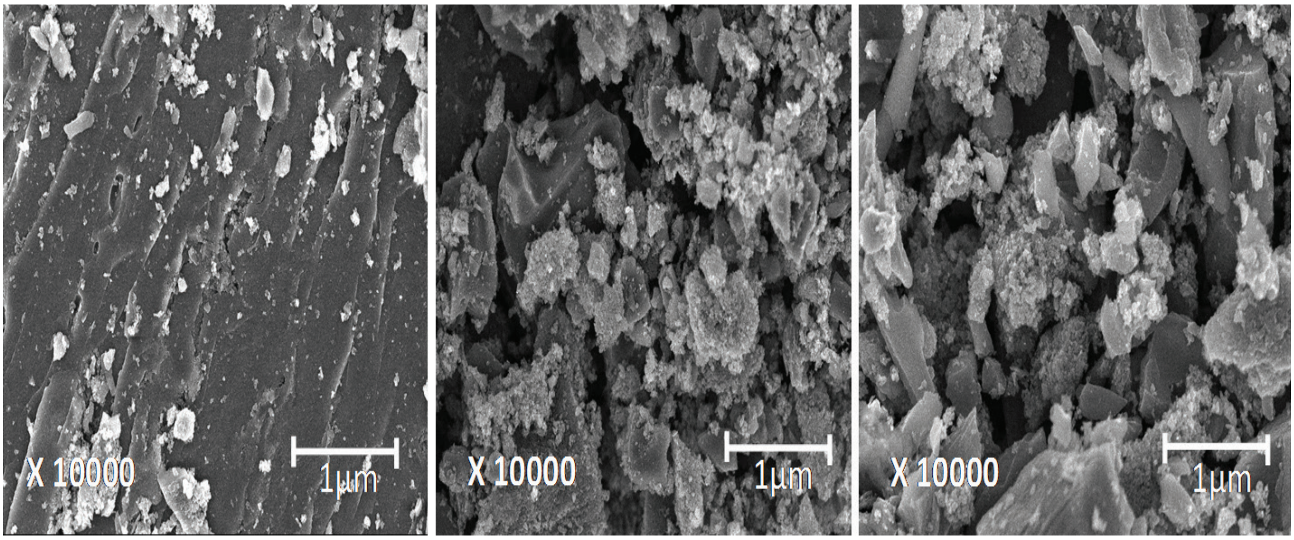

(a) (b) (c)

Fig. S2. FESEM images of AC samples: (a) AC-500, (b) AC-600, and (c) AC-CA.